Heliyon 10 (2024) e39653

Contents lists available at ScienceDirect

Heliyon

journal homepage: www.cell.com/heliyon

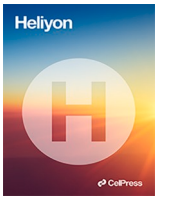

Research article

The molecular mechanisms by which the NLRP3 inflammasome regulates blood-brain barrier permeability following cryptococcal meningitis

Lingjuan Liu [a,b], Yufen Tang [a,b], Lu Zhang [a,b], Peng Huang [a,b], Xingfang Li [a,b], Yangyang Xiao [a,b], Dingan Mao [a,b], Liqun Liu [a,b], Jie Xiong [a,b,*]

[a] *Department of Pediatrics, The Second Xiangya Hospital of Central South University, Changsha, Hunan, 410011, China*
[b] *Department of Pediatric Neurology, Patientren's Medical Center, The Second Xiangya Hospital of Central South University, Changsha, Hunan, 410011, China*

ARTICLE INFO

Keywords:
Cryptococcal meningitis
NLRP3
Vimentin
Blood-brain barrier
Permeability

ABSTRACT

Objective: To investigate the mechanism underlying the regulation of blood-brain barrier permeability changes during cryptococcal meningitis by NLRP3 and Vimentin.
Methods: Sprague-Dawley rats were treated with WT Cryptococcus neoformans (Cn) or CPS1−/− Cn. Neuronal apoptosis was assessed using TUNEL staining, and pathological changes were observed using electron microscopy and HE staining. The expressions of NLRP3, Vimentin, and NF-κB in the cerebral cortex and human brain microvascular endothelial cells (HBMECs) were examined through Western blot and qRT-PCR. siNLRP3 and siVimentin were separately transfected into HBMECs, the expressions of specific factors were assessed. NF-κB and Vimentin levels were detected through immunofluorescence, apoptosis was measured using flow cytometry, and changes in the optical density (OD) of HRP were determined using ELISA.
Results: The expressions of NLRP3, Vimentin, and NF-κB were upregulated following intervention with WT Cn *in vivo* and *in vitro*. Electron microscopy revealed loose nuclear membranes in neurons and increased apoptosis in the cerebral cortex and hippocampus induced by WT Cn, accompanied by a reduction in the OD of HRP *in vitro*. siNLRP3 decreased the expressions of Vimentin, nuclear NF-κB, and β-Tubulin in HBMECs, while siVimentin downregulated total NLRP3 and nuclear NF-κB levels. Both siNLRP3 and siVimentin reduced cell apoptosis after WT Cn infection. HBMECs displayed a reduced monolayer permeability to HRP and improved cell structure arrangement.
Conclusion: Vimentin and the NLRP3 inflammasome are both implicated in the pathological process of cryptococcal meningitis. An interaction between Vimentin and the NLRP3 inflammasome is evident, likely mediated through the NF-κB signaling pathway.

1. Introduction

C. neoformans stands as the predominant causative agent of fungal meningitis in China, with a particular predilection for central nervous system (CNS) involvement [1,2]. The pathogenicity of *C. neoformans* lies in its ability to compromise blood-brain barrier (BBB)

* Corresponding author. Department of Pediatrics, The Second Xiangya Hospital of Central South University, Changsha, Hunan, 410011, China.
E-mail address: xiongjie123@csu.edu.cn (J. Xiong).

https://doi.org/10.1016/j.heliyon.2024.e39653
Received 3 February 2024; Received in revised form 19 August 2024; Accepted 21 October 2024
Available online 23 October 2024

permeability in the host, facilitating its infiltration into the CNS [3,4]. Despite extensive research, there exists no consensus on the precise mechanisms governing this process. Human brain microvascular endothelial cells (HBMECs) assume a critical role in the BBB and represent the primary route for *C. neoformans* to breach the CNS [5,6]. The integrity of HBMECs and the associated tight junctions forms the foundation of BBB formation, with cytoskeletal proteins playing a pivotal role in maintaining tight junctions [7]. Cellular tubulin comprises two closely related isoforms, α-tubulin and β-tubulin, exhibiting high structural similarity in three dimensions. These tubulins actively engage in microtubule assembly through tight dimer binding, often serving as markers for cytoskeletal structures [8]. The NLRP3 inflammasome, an integral member of the NLR (NOD-like receptor) family, assumes a critical role in the inflammatory response within the CNS. NLRP3 has been established as a key regulator of innate immunity, recognizing various pathogens and danger signals early on, thereby playing a pivotal role in thwarting foreign pathogen invasion into the CNS [9,10]. Widespread distribution characterizes NLRP3 in neurons, microglia, vascular endothelial cells, and astrocytes, with activation occurring under inflammatory conditions [11,12]. Previous studies have elucidated the induction of pathological cell death, specifically Caspase-1-dependent pyroptosis, by the NLRP3 inflammasome under inflammatory and stress conditions [13]. While its mechanism is thought to involve phagocytic cells and paracrine processes within the CNS, a unified consensus on the related processes and molecular mechanisms is yet to be reached.

Vimentin, a structural protein located in cellular intermediate filaments, plays a crucial role in the intracellular transport of cholesterol from lysosomes to specific esterification sites and is widely expressed in the CNS [14]. Prior data indicate a significant alteration in Vimentin expression in HBMECs following enterovirus 71 (EV71) intervention, suggesting its potential involvement in the modulation of BBB permeability post-viral infection. The polymerase protein of EV71 has been observed to activate the inflammasome *in vivo*, leading to the release of downstream inflammatory products and facilitating EV71 proliferation within the host [15]. Furthermore, Vimentin has been implicated in the pathogenesis of bacterial meningitis [16]. Serving as a bacterial adsorption receptor, it activates the NF-κB signaling pathway, resulting in the release of numerous inflammatory factors and exacerbating the progression of brain injury [17,18]. However, there is currently no available literature, both domestically and internationally, addressing whether *C. neoformans* meningitis triggers inflammasome activation in the host and alters Vimentin expression. Vimentin, functioning as a receptor protein, also plays a critical role in pathogen binding during the early stages of disease and in the process of virus proliferation [19]. It also plays a role in the onset and progression of various diseases through its interaction with the NLRP3 inflammasome. A deficiency in Vimentin leads to the suppression of NLRP3 inflammasome activation in the host, thereby mitigating acute lung injury and pulmonary fibrosis by decreasing the IL-1β levels in the lungs [20]. Furthermore, inhibiting the activation of the Vimentin/NLRP3/IL-1β signaling pathway has the potential to combat airway inflammation and airway remodeling associated with chronic asthma [21]. As previously discussed, the disruption and penetration of the BBB are critical steps for Cryptococcus to invade the CNS. Both Vimentin and NLRP3 inflammasomes are expressed on HBMECs and are implicated in the regulation of BBB permeability. Nevertheless, the extent to which these two factors contribute to the onset and progression of cryptococcal meningitis, as well as the underlying mechanisms, remains poorly understood.

Currently, due to the widespread use of immunosuppressants, the incidence of *C. neoformans* meningitis is steadily increasing, posing a significant threat to children's health. Despite limited research on its pathological mechanisms, the interaction between Vimentin and the inflammasome, as well as their roles in CNS infectious diseases, remains inadequately elucidated. To address this gap, our research group employed *in vivo* and *in vitro* models of cryptococcal meningitis to investigate, for the first time, the dynamic expression changes of NLRP3, Vimentin, and NF-κB in rat brains and HBMEC following *C. neoformans* infection, along with its impact on BBB permeability. In a prior phase of our study, we administered WT Cryptococcus suspension through the tail vein of Sprague-Dawley (SD) rats, collected cerebrospinal fluid (CSF) at various time points for fungal culture, and observed substantial Cryptococcus growth in the rats' CSF three days post-intervention. Consequently, we identified 3 days as an optimal time point for observation. Subsequently, we dynamically monitored the expression of each factor in brain tissue, aiming to unravel the roles and associated mechanisms of the inflammasome and Vimentin in the initiation and progression of cryptococcal meningitis.

2. Methods

2.1. Materials

The wild-type strain of *C. neoformans* (Cn) B4500FO$_2$ [22] and TYCC645#32 strain with CPS1 gene deletion [23] were selected to infect the human Brain Microvascular cells (HBMECs), which were generously provided by Huang SH (University of Southern California, Los Angeles, USA). HBMECs were procured from Sciencell Corp. (Los Angeles, USA). Fetal bovine serum and RPMI-1640 medium were obtained from Hyclone (Logan, Utah, USA), pancreatic enzymes from Gibco-BRL Corp. (Grand Island, NY, USA), and yeast, peptone, and agar from Thermo Fisher Scientific (Waltham, USA). Lipofectamine 2000 was sourced from Invitrogen Corp. (Carlsbad, CA, USA). Antibodies including HMGB1, NLRP3, NF-κB P65, and β-tubulin were purchased from Abcam Inc. (Chicago, USA), while GAPDH, PNCA, and HRP goat anti-mouse IgG were acquired from Proteintech Inc. (Chicago, USA).

2.2. C. neoforman

One soybean-sized activated WT Cn and CPS1−/− Cn colonies were individually selected from LB solid medium and then inoculated into YEPD liquid medium. Subsequently, 1 mL of organisms was extracted after 24 h of incubation in a constant temperature shaker set at 30 °C and transferred to 3 mL of YEPD medium for continued incubation under the same conditions. After an additional 24 h, the culture medium was harvested, and the supernatant was removed following centrifugation at 5000 rpm for 5 min. The

resulting pellet was washed three times with PBS for 5 min each. The concentrations of the two cryptococcus were determined using a hemocytometer and McFarland turbidimetry, respectively. The concentrations were then adjusted to 1×10^8 CFU/mL for subsequent tail vein injections in SD rats.

2.3. Animal model and treatment protocol

SD rats were procured from Changsha Ville Biological Company. Thirty-six mature SD rats were randomly divided into three groups: the normal control group, WT Cn group, and CPS1−/− Cn group. The latter two groups were administered a *C. neoformans* colony suspension through the tail vein to induce the cryptococcal meningitis model, while the control group received an equivalent dose of normal saline. Three days after tail vein injection, rats in each group were euthanized, and their brains were extracted and anesthetized via intraperitoneal injection of pentobarbital sodium. Each rat was positioned supinely, the chest was opened below the xiphoid process to fully expose the heart, and normal saline was injected through the left ventricle until the liver turned white. Subsequently, a 4 % paraformaldehyde solution was slowly injected into the left ventricle over approximately 15 min. After the entire body became rigid, the rats were decapitated, and their brains were promptly removed. Brain tissues were fixed in paraformaldehyde for 24 h. CSF and brain tissue specimens were collected, with the CSF undergoing fungal culture and the tissue specimens being embedded in paraffin. Following sectioning, HE staining was conducted to observe pathological changes in the cerebral cortex and hippocampus within each group. TUNEL fluorescence staining was employed to detect neuronal apoptosis, and changes in cerebral cortex microstructure were examined under electron microscopy. An additional six rats in each group were euthanized 3 days post-intervention, and the cerebral cortex was isolated. Total protein and RNA were then extracted, respectively. To further elucidate the dynamic changes in these factors within brain tissue following *C. neoformans* infection, another 30 SD rats were subjected to tail-vein injection with WT Cn suspension to establish the Cryptococcus meningitis model. Rats were euthanized at 0 h, 2 h, 1 d, 3 d, and 7 d intervals, every group had at least 6 rats. Subsequently, the cerebral cortex was collected, and total protein, nuclear protein, cytoplasmic protein, and total RNA were extracted, respectively.

2.4. HE staining

The rat brain tissue sections were incubated at 60 °C for 1–2 h in an incubator. Following this, the sections were dewaxed in water. The tissue sections underwent a sequential process, starting with a 10-min immersion in xylene, followed by exposure to varying concentrations of ethanol. They were then washed with distilled water, stained with hematoxylin for 5–10 min, stained with eosin for 3–5 min, and finally rinsed with distilled water. Dehydration was carried out using gradient concentrations of alcohols for 5 min each. After two rounds of 10-min soaking in xylene, the sections were mounted with neutral gum, and tissue morphology changes were observed under the microscope (BA210T, Motic, China).

2.5. Cell culture and transfection

HBMECs were cultured in RPMI 1640 complete medium in a 5 % CO_2 incubator at 37 °C. The cells were divided into three groups: the control group, WT Cn group, and CPS1−/− Cn group. In the intervention group, WT Cn (10^5/mL) and CPS1−/− Cn (10^5/mL) suspensions were separately added, and the intervention was terminated after a 24-h cell incubation. The control group received an equivalent dose of PBS.

For *in vitro* cell culture, 5 μL of NLRP3/Vimentin-siRNA-1 and 5 μL of Lip2000 were used. NLRP3/Vimentin-siRNA-2, NLRP3/Vimentin-siRNA-3, and NC were added to six additional centrifuge tubes following the same method, standing at room temperature for 20 min. After a 6-h incubation in a 37 °C incubator, the medium was replaced with fresh complete medium. After 48 h of transfection, cells were washed with PBS, lysed with lysis buffer for 10 min, and then centrifuged at 4 °C, 12,000 rpm for 15 min. The resulting supernatant was stored at −20 °C for later use. Table 2 provides the siRNA sequences for specific factors.

2.6. Flow cytometry

The HBMECs in each group were harvested using trypsin digestion solution without EDTA. The cells were rinsed twice with PBS, followed by centrifugation at 2000 rpm for 5 min each cycle, resulting in the collection of approximately 5×10^5 cells. Subsequently, a

Table 1
The primer sequences.

Primer sequences	
GAPDH-F	ACAGCAACAGGGTGGTGGAC
GAPDH-R	TTTGAGGGTGCAGCGAACTT
NF-κB-F	CACCAAAGACCCACCTCACCG
NF-κB-R	CTTGCTCCAGGTCTCGCTTC
NLRP3-F	CACCTCTTCTCTGCCTACCTG
NLRP3-R	AGCTGTAAAATCTCTCGCAGT
Vimentin-F	AGTCAAACGAATACCGGAGACA
Vimentin-R	AATTCTCTTCCATTTCACGCATC

sequential addition of 500 μL of Binding buffer to suspend the cells, followed by 5 μL of Annexin V-FITC, was performed. Then, 5 μL of Propidium Iodide was added and thoroughly mixed. The resulting mixture was incubated at room temperature in darkness for 15 min. Finally, it was analyzed using flow cytometry within 1 h.

2.7. Western blot analysis

Total protein was extracted from cerebral cortex and HBMECs using RIPA lysis buffer (Applygen, Beijing, China), and the protein concentration was determined with a protein detection kit (TransGen Biotech, Beijing, China). The primary antibodies employed in this study included Vimentin (ab8978, Abcam, UK, 1:500), NLRP3 (19771-1-AP, Proteintech, US, 1:500), NF-KB P65 (ab16502, Abcam, UK,1:1000), GAPDH (10494-1-AP, Proteintech, US, 1:4000) and PCNA (60097-1-Ig, Proteintech, US, 1:7000. ECL (Tiangen Biochemical Technology, Beijing, China) was utilized to detect immunoreactive bands thorough Bio-Rad gel imaging System (California, USA) following incubation with the corresponding horseradish peroxidase-conjugated secondary antibodies.

2.8. Quantitative real-time PCR

Total RNA from both the hippocampus and HBMECs was isolated using Trizol reagent (Invitrogen, Carlsbad, CA, USA) following established procedures. Subsequently, 1 μg of RNA was reverse transcribed to cDNA using oligo (dT) primers. qRT-PCR assays were conducted for NLRP3, Vimentin, NF-κB (RiboBio, Guangzhou, China), along with GAPDH mRNA (RiboBio, Guangzhou, China). The $2^{-\triangle\triangle CT}$ method was employed to determine the relative expression levels of specific factors normalized to GAPDH. Table 1 provides the primer sequences for specific factors and GAPDH.

2.9. BBB permeability studies

Confluent monolayers of HBMECs were apically incubated with assay buffer. In both the control and experimental groups, the transwell chambers were supplemented with 50 μL of PBS and 50 μL of *C. neoformans* strains at a concentration of 1 × 10^6 CFU/mL, respectively. At 24-h intervals, HBMECs were removed from the incubator and washed three times with PBS. For the incubation step, 500 μL of medium mixed with HRP (P6782, Sigma-Aldrich, USA, 1:500) was added to the upper chamber for 30 min, while only 1.5 mL of medium was added to the lower chamber. At various time points, 60 μL samples were collected from the chambers and plated onto a 96-well plate. HBMECs were then treated with 5 % TMB for 10 min, and the reaction was stopped with 0.36 mol/L sulfuric acid. Finally, the optical density of HRP was measured by ELISA at a wavelength of 450 nm.

2.10. Immunofluorescence microscopy

The HBMECs slides underwent a fixation step using 4 % paraformaldehyde for 30 min, followed by a PBS rinse. Subsequently, 0.3 % Triton was added for permeabilization at 37 °C over 30 min. Post-permeabilization, the slides were washed thrice with PBS for 5 min each and then exposed to 5 % BSA at 37 °C for 60 min. Next, appropriately diluted primary antibodies (Vimentin (ab8978, Abcam, UK, 1:100) + NF-κB (ab16502, Abcam, UK,1:200)) or β tubulin (ab18207, Abcam, UK,1:100) were applied and left overnight at 4 °C. Afterward, the slides were washed three times with PBS for 5 min each. Subsequently, 50–100 μL of secondary antibody was applied, followed by a 90-min incubation at 37 °C. The slides were then rinsed again thrice with PBS for 5 min each time. For nuclear staining, DAPI working solution was applied at 37 °C for 10 min, followed by a PBS wash for 5 min. Finally, the slides were mounted using buffered glycerol, repeating the process three times. The stained slides were directly observed under a fluorescence microscope (Nikon eclipseE400, Nikon Corporation, Japan), and images were captured.

2.11. Enzyme Linked Immunosorbent Assay (ELISA)

The cells were seeded in collagen-coated transwell wells to form a monolayer, achieving confluence within 2–3 days. In the control group, 50 μL of PBS was added to the transwell. The Cn group received 50 μL of a 1 × 10^6 CFU/mL bacterial solution, resulting in a final concentration of 10^5 CFU/mL. The cultures were maintained in a 5 % CO_2 incubator at 37 °C. After 24 h of incubation, cells were washed with PBS, and 500 μL and 1.5 mL of cell culture medium were added to the upper chamber. Subsequently, a 1:500 diluted HRP solution was applied for 30 min. From each well, 60 μL of liquid was extracted from the lower chamber and transferred to a 96-well

Table 2
The siRNA sequences.

siRNA sequences	
Vimentin siRNA-1	GCAGAAGAATGGTACAAAT
Vimentin siRNA-2	CAACGAAACTTCTCAGCAT
Vimentin siRNA-3	CCATCAACACCGAGTTCAA
NLRP3 siRNA-1	GGATCAAACTACTCTGTGA
NLRP3 siRNA-2	GAGAGACCTTTATGAGAAA
NLRP3 siRNA-3	GGGACACTCTACCAAGACA

plate. Following this, a 1:20 diluted TMB solution was added for a 10-min incubation. The optical density (OD) of HRP was measured using a microplate reader at a wavelength of 450 nm.

2.12. Statistical analysis

We conducted data analysis using SPSS 22.0 statistical software and expressed the results as means ± SEM. Multiple comparisons were performed using one-way analysis of variance (ANOVA) followed by the LSD post hoc test. Pearson correlation analysis was utilized for correlation assessments. Statistical significance was set at p values < 0.05 in the current experiments. Each experiment was repeated three times for robustness and reliability.

3. Results

3.1. Establishment of a rat cryptococcal meningitis model and changes in its tissue structure

The rat cryptococcal meningitis model was successfully established, as evidenced by the growth of yellow-white round colonies in

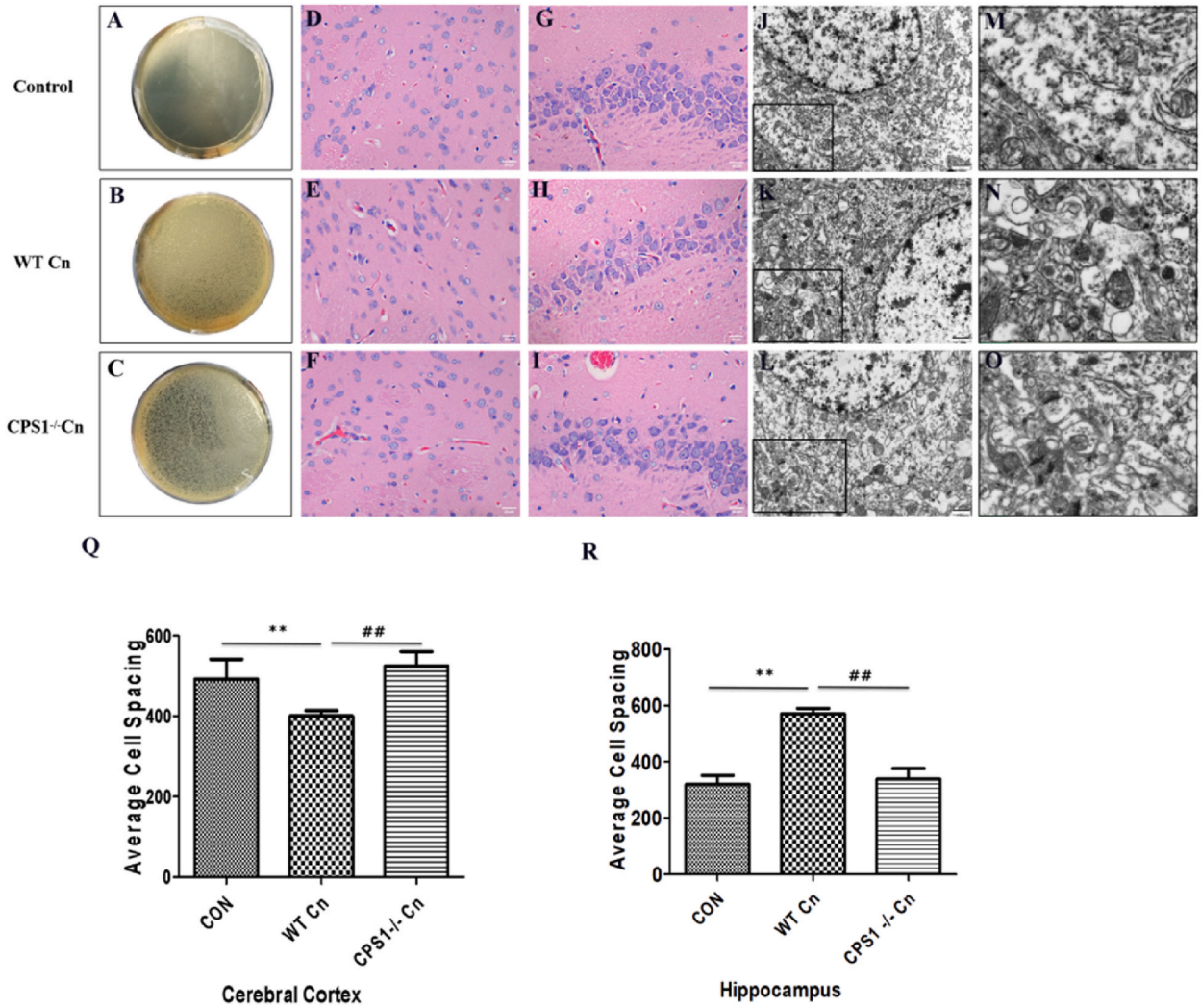

Fig. 1. Establishment of a rat cryptococcal meningitis model and changes in its tissue structure (n = 6). Five to seven days post-cultivation of CSF from both the WT Cn group and the CPS1−/− Cn group, yellow-white round colonies were discernible on the agar plates (A–C). HE staining revealed distinct alterations in the cerebral cortex (D–F) and hippocampus (G–I) subsequent to Cryptococcus intervention. Panels J–O depict electron microscopic variations observed across the different experimental groups (× 400). Image J software was employed to analyze the mean cell spacing of the cerebral cortex (Q) and hippocampus (R) in HE staining. Statistical comparisons, denoted as $^{**}P < 0.001$, were made relative to the control group, while comparisons with the WT Cn group were indicated as $\#\#P < 0.001$.

the CSF of both the WT Cn group and the CPS1−/− Cn group 5–7 days post-culturing. These colonies, appearing moist and transparent, indicated that Cryptococcus neoformans could effectively traverse the BBB and proliferate within the host's CSF. Quantitative analysis revealed a significantly higher number of CSF colonies in the WT Cn group compared to both the control group and the CPS1−/− Cn group (Fig. 1A–C).

Histological examination using HE staining demonstrated clear neuronal structures in the rat cerebral cortex and hippocampus of the control group. Cells exhibited intact and continuous cell walls, light blue nuclei with uniform staining (Fig. 1D–I). In contrast, neurons in the WT Cn-infected group displayed characteristics such as more loosely arranged in the hippocampus (Fig. 1R), while the space between cells narrowed (Fig. 1Q), irregular shape, partial nuclear fragmentation, dissolution, pyknosis, hyperchromatism, and increased vacuoles. Following intervention with CPS1−/− Cn, alterations in neuron morphology were noted, although significantly less pronounced compared to the WT Cn group. The cell arrangement remained relatively regular.

Ultrastructural analysis using electron microscopy in the control group revealed evident cytoplasmic euchromatin in cerebral cortex neurons, reduced heterochromatin, a smooth and intact nuclear membrane, evenly distributed nucleoplasm, and abundant, regularly arranged organelles. These findings highlight the structural integrity of neurons in the absence of infection.

Following Cryptococcus intervention, notable alterations in neuronal ultrastructure were observed, including a loose and discontinuous nuclear membrane, clustered nucleoplasm, disordered arrangement of cytoplasmic organelles, a significant reduction in the endoplasmic reticulum and Golgi apparatus, aggregation of mitochondria, and a marked increase in vacuoles (Fig. 1J–O).The apoptosis of neurons exhibited a significant increase in the WT Cn group, particularly in cells closer to the cortex. In the aftermath of *C. neoformans* infection, apoptosis in hippocampal neurons was less pronounced compared to that in the cerebral cortex. Notably, CPS1−/− Cn intervention also accelerated neuronal apoptosis in the cerebral cortex of rats, though the apoptosis rate in the hippocampus did not reach statistical significance when compared with the control group (Fig. 2A and B).

3.2. Expression changes of NLRP3, Vimentin and NF-κB in rat cerebral cortex and HBMECs after C. neoformans meningitis

The protein levels (Fig. 3A) and mRNA levels (Fig. 3B) of NLRP3, Vimentin, and NF-κB in the cerebral cortex of SD rats following WT Cn intervention were significantly up-regulated compared to the control group and CPS1−/− Cn group (Fig. 3A, C and 3D). The protein expression levels of these factors after CPS1−/− Cn intervention showed no significant difference from those in the control group. Following WT Cn intervention, the expressions of total Vimentin, NLRP3, total NF-κB, and nuclear NF-κB gradually increased at 2 h, peaked at 3 d, and then gradually decreased at 7 d. Similarly, the protein level of Vimentin in the cytoplasm also began to up-regulate in the early stages after *C. neoformans* intervention, peaked at 3 d, and gradually decreased at 7 d (Fig. 3E–G). Additionally, qRT-PCR analysis revealed that mRNA levels of Vimentin, NLRP3, and NF-κB increased at 2 h after *C. neoformans* infection,

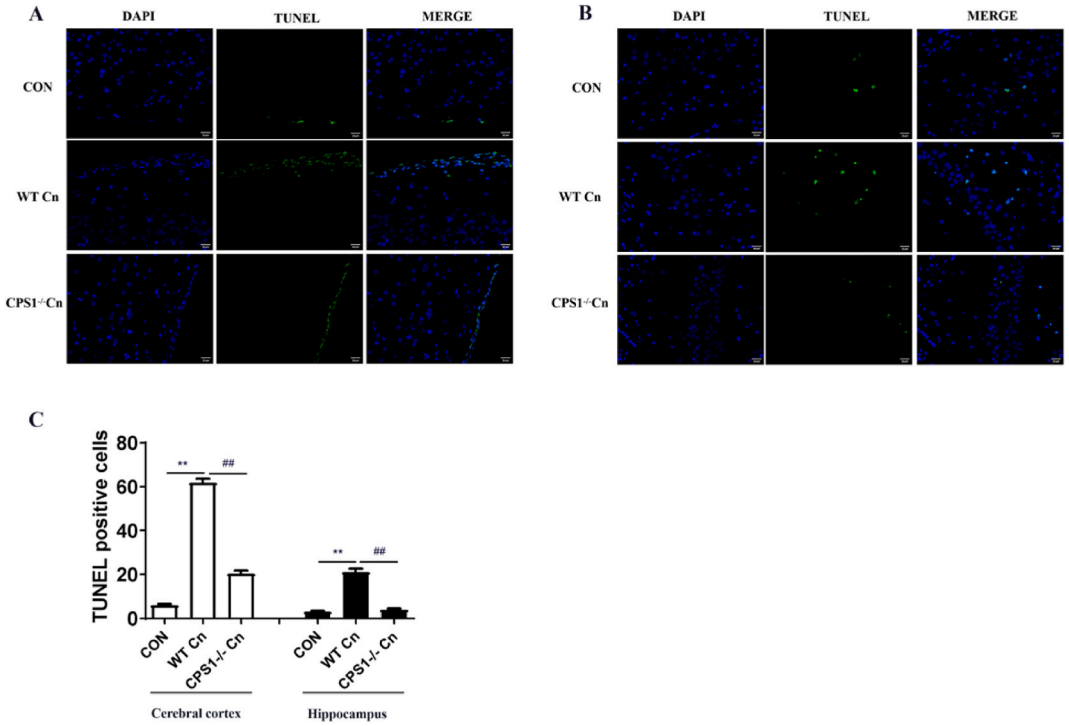

Fig. 2. The effects of C.neoformans on neurons apoptosis in cerebral cortex (A)and hippocampus (B) of SD rats. Green fluorescence represents apoptosis cells.In Figure C, the number of TUNEL-positive cells each group is depicted (× 400).The bar graphs display the means ± SEM (n = 6). Compared to the control group,$^{**}P < 0.001$, while comparisons with the WT Cn group were indicated as $\#\#P < 0.001$.

peaked at 3 d, and then gradually decreased at 7 d (Fig. 3H).

Consistently, the protein levels of NLRP3, Vimentin, and NF-κB were significantly up-regulated following 24 h of WT Cn intervention *in vivo*, whereas CPS1−/− Cn had minimal effects on these factors (Fig. 3I). qRT-PCR analysis also revealed a nearly 4.2-fold up-regulation in NF-κB mRNA levels, approximately 2.3 times increase in NLRP3 mRNA expression, and a 1.5-fold up-regulation in Vimentin mRNA levels after 24 h of WT Cn intervention (Fig. 3J–L). In comparison to the control group, nuclear NF-κB expression was up-regulated after CPS1−/− Cn intervention, while NLRP3 and Vimentin mRNA levels showed no significant changes.

Immunofluorescence studies further demonstrated that *C. neoformans* significantly increased the expressions of Vimentin and NF-κB in the cytoplasm *in vitro*, accelerating the nuclear translocation of NF-κB (Fig. 3M). Additionally, cell apoptosis was significantly up-regulated after *C. neoformans* infection (Fig. 3O), leading to a remarkable increase in the OD of HRP (Fig. 3N). These findings indicate that Cryptococcus exacerbates apoptosis in HBMECs, compromises BBB permeability, and contributes to a progressive increase in brain damage.

3.3. The effects of NLRP3 on vimentin expression in HBMECs after C. neoformans infection

Three siNLRP3 sequences were designed and transiently transfected into HBMECs. The impact of siNLRP3 expression was assessed using Western blot and qRT-PCR analyses (Fig. 4A). In comparison to the control group, all three siRNA sequences led to a significant reduction in NLRP3 protein and mRNA levels *in vivo*, confirming the success of transfection. Notably, siNLRP3-3 exhibited the most pronounced down-regulation of NLRP3 expression, and therefore, it was chosen for subsequent experiments. SiNLRP3 transfection not only suppressed NLRP3 protein expression in HBMECs but also markedly decreased the levels of total Vimentin and nuclear NF-κB proteins. Following the inhibition of NLRP3 inflammasome activation, the expressions of total Vimentin and nuclear NF-κB proteins in HBMECs infected with Cryptococcus were significantly reduced (Fig. 4B).

Consistently, immunofluorescence analysis demonstrated that siNLRP3 significantly reduced the cytoplasmic expressions of Vimentin and NF-κB *in vitro*, concurrently inhibiting NLRP3 expression in the cells. This resulted in a substantial reduction in the up-regulation of Vimentin induced by *C. neoformans* infection, a decrease in the expression of NF-κB in the nucleus, and an inhibition of NF-κB nuclear translocation. Moreover, the fluorescence level of NF-κB in the cytoplasm was significantly down-regulated after siNLRP3 intervention (Fig. 4C).

3.4. Effects of NLRP3 on apoptosis and permeability of HBMECs after C. neoformans infection

The protein level of β-Tubulin in HBMECs was notably decreased following siNLRP3 pretreatment. After 48 h of WT Cn intervention, the β-Tubulin protein level in HBMECs was significantly higher than that in the control group. However, the elevated β-Tubulin expression induced by Cryptococcus was significantly mitigated after siNLRP3 intervention (Fig. 4B). Immunofluorescence results depicted a clear cytoskeleton in normal HBMECs, with β-Tubulin evenly distributed in the cytoplasm and minimal expression in the nucleus. Following WT Cn intervention, cells exhibited obvious shrinkage, compact and pyknotic β-Tubulin arrangement, unclear structure, and reduced cell size. NLRP3 inhibition partially alleviated these changes (Fig. 4D).

Furthermore, cell apoptosis was slightly lower after siNLRP3 pretreatment, whereas HBMEC apoptosis significantly increased after WT Cn intervention (Fig. 4E). Inhibition of NLRP3 significantly decreased HBMEC apoptosis and the OD of HRP after *C. neoformans* infection (Fig. 4F).

3.5. Effects of vimentin on HBMEC apoptosis and permeability in HBMECs after C. neoformans infection

Three siVimentin sequences were individually transfected into *in vitro*-cultured HBMECs. All three siRNA sequences demonstrated a significant down-regulation of Vimentin levels, confirming successful transfection (Fig. 5A). Among them, siVimentin-1 exhibited the most pronounced down-regulation of mRNA expression post-transfection, prompting its selection for subsequent experiments. Results indicated that siVimentin significantly reduced NLRP3 expressions in HBMECs, and it effectively decreased the NLRP3 inflammasome induced by Cryptococcus infection. Furthermore, siVimentin alleviated nuclear NF-κB protein and mRNA levels in HBMECs, suggesting that Vimentin plays a role in inhibiting the activation of the NF-κB signaling pathway *in vitro* (Fig. 5B).

Flow cytometry analysis revealed a significant reduction in HBMEC apoptosis *in vitro* following siVimentin treatment. The inhibition of Vimentin led to a notable alleviation of Cryptococcus-induced HBMEC apoptosis (Fig. 5C). Additionally, the OD of HRP was significantly lower post siVimentin transfection compared to the normal control group. The elevated OD to HRP induced by Cryptococcus infection was significantly attenuated after siVimentin intervention (Fig. 5D).

4. Discussion

Cryptococcal meningitis is prevalent in children, typically following a subacute course marked by an insidious onset, prolonged duration, and numerous sequelae, posing a serious threat to children's health [24]. The proliferation of Cryptococcus in the CNS, achieved by breaching the host's BBB, constitutes a crucial aspect of its pathogenesis [25]. The capsule, identified as a key virulence factor of *C. neoformans*, plays a pivotal role in the penetration of HBMECs. Its mechanism is associated with the activation of specific receptors or signaling pathways on endothelial cells [26]. In this study, we intravenously injected wild-type Cryptococcus and Capsule-knockout Cryptococcus into SD rats, respectively. The results demonstrated that both fungal strains could be cultured in the host's CSF, and both entered the CNS by breaching the host's BBB. This implies that the capsule may not be indispensable for

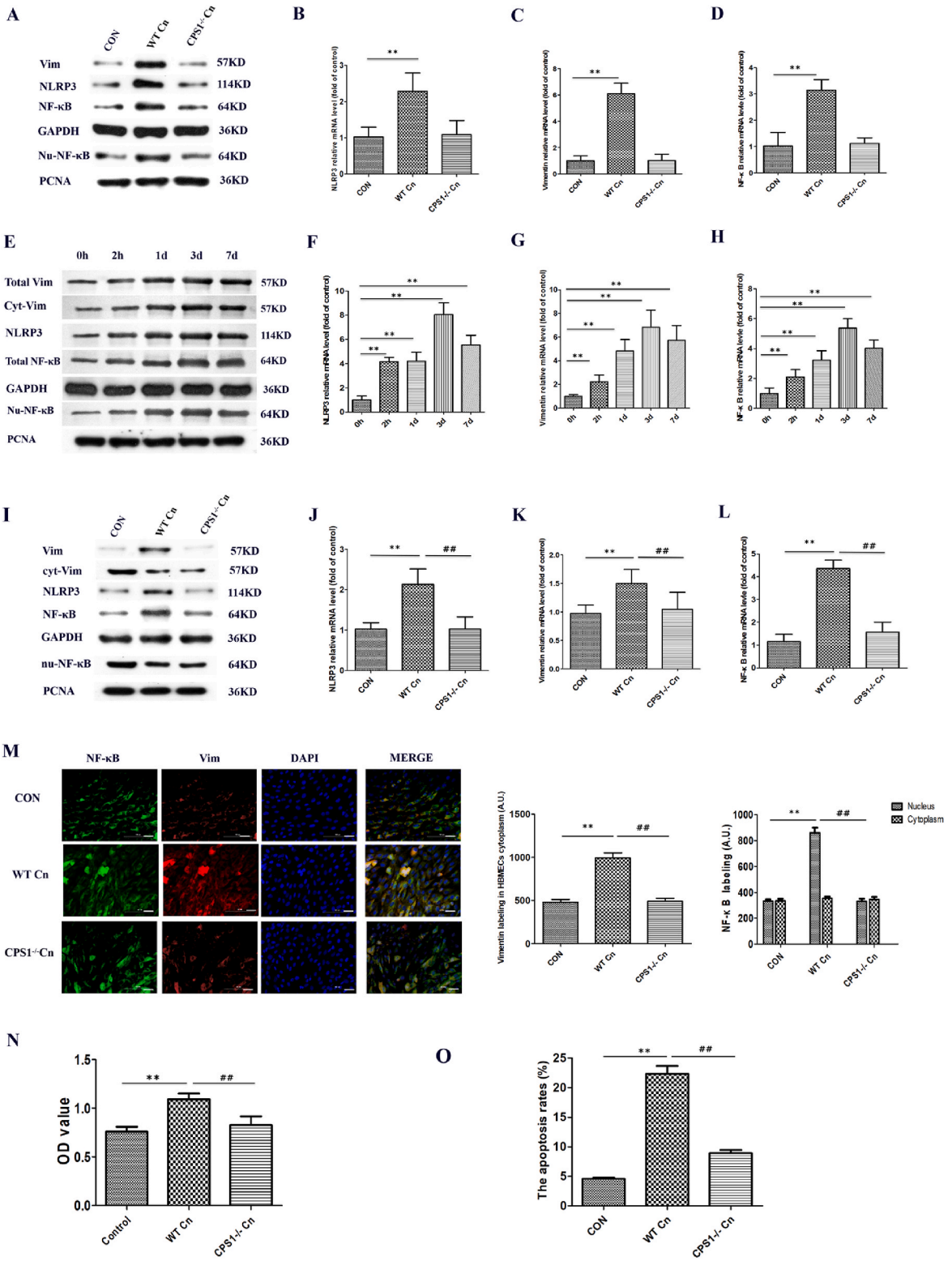

Fig. 3. Expression changes of NLRP3, Vimentin and NF-κB in rat cerebral cortex and HBMECs after *C. neoformans* infection. The protein expressions of NLRP3, Vimentin, and NF-κB, as well as mRNA levels (A, B-D), were assessed in the rat cerebral cortex of each experimental group using Western blot and qRT-PCR, respectively. Dynamic alterations in NLRP3, Vimentin, and NF-κB protein expressions (E) and mRNA levels (F–H) were observed *in vivo* (n = 6). Furthermore, the expressions of NLRP3, Vimentin, and NF-κB proteins (I) and mRNA levels (J–L) were investigated in HBMECs. Immunofluorescence analysis (M) demonstrated the impact of *C. neoformans* on NF-κB and Vimentin expressions in HBMECs (n = 3). The influence

of *C. neoformans* on HBMEC apoptosis was evaluated through flow cytometry (N) (× 400). Changes in HRP permeability in HBMEC monolayers post-*C. neoformans* infection were examined (O). Statistical comparisons, denoted as $^{**}P < 0.001$, were made relative to 0 h (F–G) or the control group, while comparisons with the WT Cn group were indicated as $\#\#P < 0.001$.

C. neoformans to traverse the BBB. Subsequently, we examined the impact of these two different types of Cryptococcus on neuronal apoptosis in the rat cerebral cortex and hippocampus. The findings revealed that *C. neoformans* led to a significant increase in neuronal apoptosis, primarily in the cerebral cortex, with less involvement in the hippocampus, which suggests that the cerebral cortex is the most frequently affected area following Cryptococcus infection. Furthermore, decapsulated Cryptococcus had minimal effects on the pathological morphology of the rat hippocampus but still exacerbated neuronal apoptosis in the cerebral cortex. This effect could be attributed to other virulence factors of Cryptococcus, including hyaluronic acid, melanin, urease, and other factors.

Additionally, our data have confirmed that the disruption of BBB permeability induced by *C. neoformans* infection is associated with the NLRP3, Vimentin, and NF-κB signaling pathways. Cryptococcus activates the NLRP3 inflammasome both *in vivo* and *in vitro*, inducing the expression of Vimentin and subsequently activating the NF-κB signaling pathway. The NLRP3 inflammasome, a multi-protein complex, plays a crucial role, as its deficiency can reduce HBMEC permeability and inhibit microglia activation in the CNS. This leads to a significant reduction in ischemic lesions after middle cerebral artery occlusion, potentially through the inhibition of IL-1β release mediated by the activation of the NLRP3 inflammasome [27]. Moreover, Fann et al. have demonstrated that interventions such as intermittent fasting or intravenous immunoglobulin can variably inhibit the activation of the NLRP3 inflammasome *in vivo*, subsequently reducing neuronal apoptosis after ischemic stroke and promoting the recovery of motor function [28]. In animal models of cerebral hemorrhage, the activation of the NLRP3 inflammasome has been found to expedite the inflammatory response by stimulating the release of IL-1 and the infiltration of neutrophils [29]. However, the level of myeloperoxidase in the CNS significantly decreases after NLRP3 knockout, substantially alleviating the degree of brain edema. Recent studies have highlighted melatonin's ability to inhibit the activation of the NLRP3 inflammasome, consequently reducing the release of IL-1β and IL-18. This inhibition has shown promising results in significantly improving neuronal damage after subarachnoid hemorrhage, exerting a neuroprotective effect [30].

Furthermore, NLRP3 activation has been implicated in increasing BBB extravasation, hastening the degradation of tight junction proteins, and exacerbating neuronal apoptosis following CNS injury [31]. The initiation and activation processes play pivotal roles in regulating the NLRP3 inflammasome, with the former primarily mediated by the NF-κB signaling pathway. Certain pathological factors expedite the translocation of NF-κB from the cytoplasm to the nucleus, thereby promoting NLRP3 secretion and Caspase-1 maturation, triggering an immune response in the host [32]. In the context of bacterial meningitis, the activation of nuclear translocation of NF-κB in the CNS has been observed. Inhibiting NF-κB activation has shown promise in combating transient focal cerebral ischemia induced by CNS inflammation, thereby reducing the extent of brain damage [33]. The role of the NF-κB signaling pathway in BBB permeability has garnered increased attention. Wang et al. recently demonstrated that hypertonic saline reduces IL-1β release by inhibiting NLRP3 inflammasome activation in glial cells. This inhibition subsequently lowers the phosphorylation level of NF-κB P65 and the expression of vascular endothelial growth factor on astrocytes, ultimately enhancing BBB permeability and reducing brain infarct volume [34]. Our current study confirms that cryptococcal meningitis activates the NLRP3 inflammasome and the NF-κB signaling pathway both *in vivo* and *in vitro*. This activation disrupts BBB integrity, exacerbates neuronal apoptosis, and thereby worsens the invasion of Cryptococcus into the CNS. These effects may be linked to the amplification of inflammatory responses. After inhibiting NLRP3, the expression of NF-κB notably diminished. The use of siNLRP3 significantly curtailed the translocation of cytoplasmic NF-κB protein into the nucleus, thus impeding the activation of the NF-κB signaling pathway subsequent to *C. neoformans* infection. This action alleviated apoptosis and preserved the normal cytoskeletal structure. Ultimately, siNLRP3 intervention mitigated the condensation of HBMECs, safeguarded the integrity of the BBB, and mitigated the invasion of Cryptococcus into the CNS.

Recent studies have demonstrated the involvement of Vimentin in mediating inflammasomes leading to conditions such as bacterial meningitis and pulmonary edema in mice [35]. In the context of CNS infection, EV71 may induce inflammasome activation through Vimentin, promoting Caspase-1 activation, IL-1β release, and exacerbating neuronal apoptosis [36]. Additionally, Vimentin plays a role in glial scar formation, serving as protein carriers for various cells and participating in the regulation of cell movement, migration, and proliferation. The absence of Vimentin upregulates CNS synaptic plasticity, post-traumatic glial regeneration, and accelerates the recovery of neuromotor function after brain injury [37]. Silencing Vimentin in glioma cells using RNAi restricts the growth of reactive astrocytes, weakens mitochondrial biological activity, accelerates neurological function recovery after spinal cord injury, and reduces the occurrence of sequelae [38]. To further explore the relationship between Vimentin and the NLRP3 inflammasome, siNLRP3 or siVimentin was transfected into HBMECs in the present study. The results revealed that siNLRP3 significantly reduced the protein and mRNA expression levels of Vimentin in HBMECs, leading to a significant down-regulation of elevated Vimentin levels induced by Cryptococcus infection. Silencing Vimentin in HBMECs resulted in a significant decrease in the expression level of NLRP3 *in vitro*. Furthermore, the nuclear translocation of NF-κB was significantly reduced, thus resisting apoptosis induced by Cryptococcus infection and maintaining the integrity of the BBB. Therefore, it is plausible to posit that wild-type Cryptococcus can induce HBMECs to secrete a substantial amount of Vimentin, subsequently activating the NF-κB signaling pathway. This activation, in turn, prompts cells to generate a significant quantity of the pro-inflammatory factor NLRP3, amplifying the inflammatory response in host cells, accelerating HBMEC apoptosis, and causing severe damage to BBB integrity. The expression of Vimentin is regulated by the NF-κB signaling pathway, which can bind to regulatory elements in the promoters of the Vimentin-encoding genes, influencing protein expression.

However, findings by Huang et al. suggest that Vimentin, when activated by the NF-κB signaling pathway, accelerates neutrophil

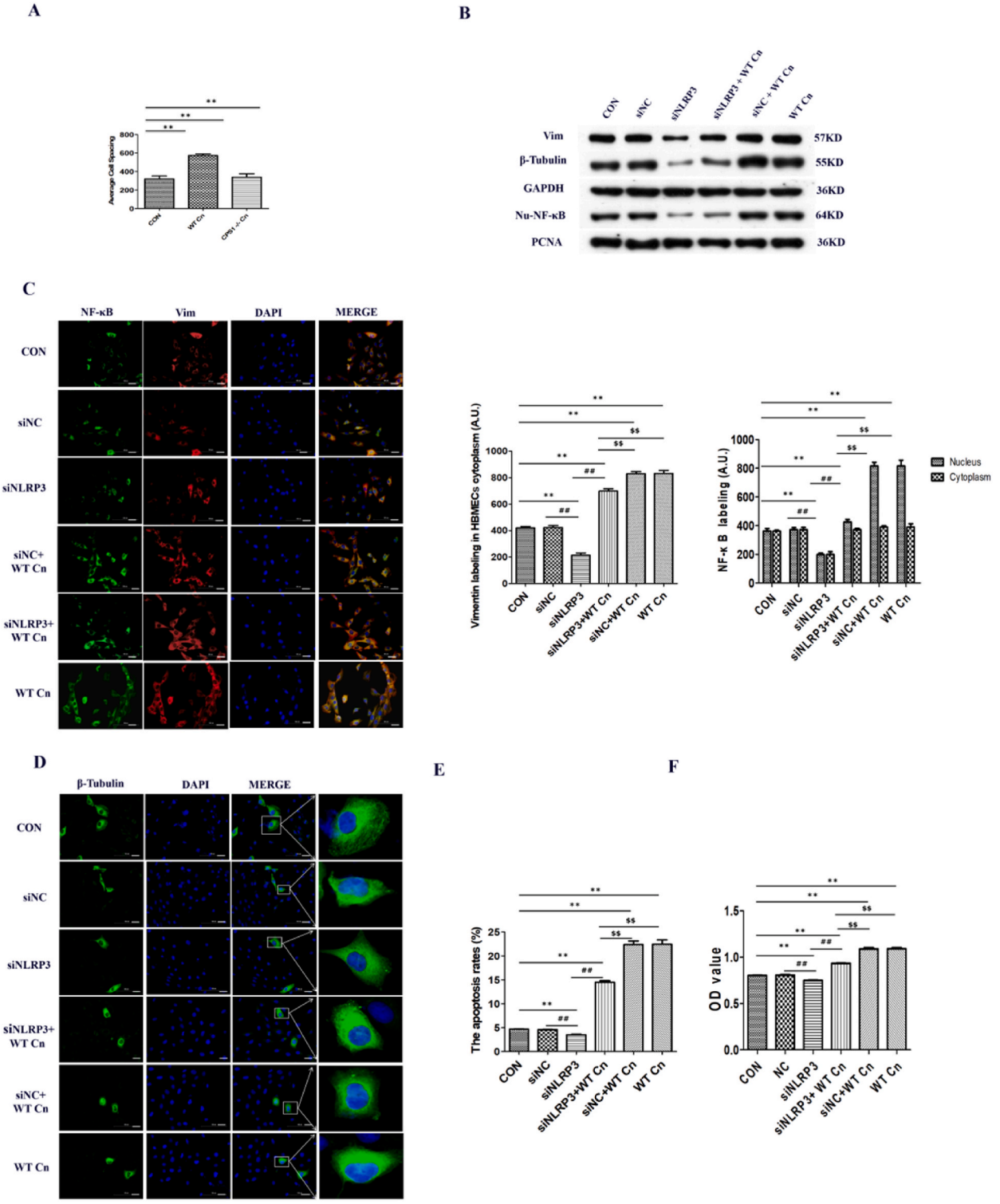

(caption on next page)

Fig. 4. The effects of NLRP3 on apoptosis and permeability of HBMECs after *C. neoformans* infection (n = 3). The impact of siNLRP3 expression was assessed using Western blot and qRT-PCR (A). The influence of NLRP3 on Vimentin, β-Tubulin, and NF-κB (both total and nuclear) proteins in HBMECs following *C. neoformans* infection was examined through Western blot (B) and immunofluorescence (C). NLRP3's effect on HBMEC structure after *C. neoformans* infection was visualized using immunofluorescence (D) (× 400). The impact of NLRP3 on HBMEC apoptosis post-*C. neoformans* infection was quantified through flow cytometry (E). Changes in HRP permeability in HBMECs mediated by NLRP3 after *C. neoformans* infection were evaluated (F). Statistical comparisons, denoted as $^{**}P < 0.001$, were made relative to the control group, while comparisons with the siNLRP3 group were indicated as $\#\#P < 0.001$, and comparisons with the siNLRP3 + WT Cn group were indicated as $\$\$P < 0.001$.

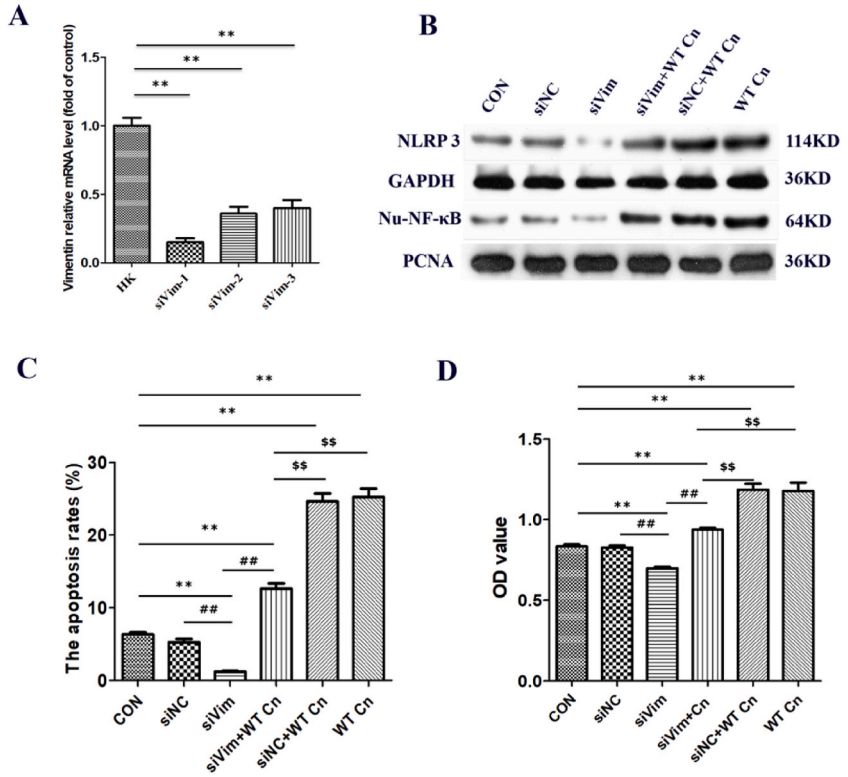

Fig. 5. The effects of Vimentin on apoptosis and permeability of HBMECs after *C. neoformans* infection (n = 3). The impact of siVimentin expression was assessed through qRT-PCR (A). The influence of Vimentin on NLRP3 and nuclear NF-κB proteins in HBMECs following *C. neoformans* infection was examined via Western blot (B). Vimentin's effects on HBMEC apoptosis post-*C. neoformans* infection were quantified using flow cytometry (C). Changes in HRP permeability in HBMECs mediated by Vimentin after *C. neoformans* infection were evaluated (D). Statistical comparisons, denoted as $^{**}P < 0.001$, were made relative to the control group, while comparisons with the siVim group were indicated as $\#\#P < 0.001$, and comparisons with the siVim + WT Cn group were indicated as $\$\$P < 0.001$.

recruitment and aggregation, disrupts BBB permeability, and exacerbates damage to the pathogenic CNS [39]. Our present study also revealed that inhibiting Vimentin could diminish the activation of the NF-κB signaling pathway *in vitro*. This reduction not only mitigated brain damage but also regulated cellular immune function following *C. neoformans* infection. These findings imply that the Vimentin/NF-κB signaling pathway might play a bidirectional role in CNS infection-induced brain injury. On one hand, NLRP3 inflammasome activation post Cryptococcus infection induces Vimentin expression in the CNS, subsequently activating the NF-κB signaling pathway. This activation results in increased BBB permeability, accelerating Cryptococcus entry into the CNS, aggravating neuronal apoptosis, and ultimately leading to irreversible pathological brain damage. Additionally, Vimentin negatively regulates the activation of the NLRP3 inflammasome. The suppressive influence of the NLRP3 inflammasome on Vimentin may be mediated through NF-κB. Consequently, this mechanism could also be linked to the downregulation of NF-κB expression within host cells. Indeed, the interplay among these three cytokines is intricate and multifaceted. *In vivo* studies have shown that inhibiting both the activation of the NLRP3 inflammasome and the expression of Vimentin can substantially mitigate brain injury following *C. neoformans* infection. This underscores a novel avenue for future research in the development of innovative antifungal treatments.

5. Conclusion

The current study elucidates the involvement of Vimentin, the NLRP3 inflammasome, and the NF-κB signaling pathway in the

progression of Cryptococcal meningitis. Cryptococcal meningitis induces the activation of the NLRP3 inflammasome and an upregulation of Vimentin in the CNS, leading to accelerated apoptosis of HBMECs and disruption of BBB integrity. Furthermore, the interaction between Vimentin and the NLRP3 inflammasome appears to be facilitated through the NF-κB signaling pathway. The *in vitro* and *in vivo* models presented in this study are poised to contribute to a more comprehensive understanding of the molecular underpinnings of *C. neoformans*, specifically regarding endothelial cell apoptosis and inflammatory responses. These findings may offer a novel theoretical foundation for the development of treatments for fungal infections in the future.

CSF: cerebrospinal fluid, BBB: blood-brain barrier, HBMEC: human brain microvascular endothelial cell, CNS: central nervous system, EV71: enterovirus 71, ELIS A: Enzyme Linked Immunosorbent Assay, OD: optical density, ANOVA: One-way analysis of variance.

CRediT authorship contribution statement

Lingjuan Liu: Writing – review & editing, Writing – original draft, Conceptualization. **Yufen Tang:** Writing – review & editing, Writing – original draft. **Lu Zhang:** Methodology, Data curation. **Peng Huang:** Investigation, Data curation. **Xingfang Li:** Formal analysis. **Yangyang Xiao:** Methodology. **Dingan Mao:** Conceptualization. **Liqun Liu:** Conceptualization. **Jie Xiong:** Methodology, Formal analysis.

Ethics approval and consent to participate

This study was approved by the Ethics Committee, the Second Xiangya Hospital, Central South University, China (Ethics Batch number: 2020400, Experimental Animal Use License: SYXK (Xiang) 2017–0002).

Conflict of interest

The authors declare that the research was conducted in the absence of any commercial or financial relationships that could be construed as a potential conflict of interest.

Data availability statement

The original contributions presented in the study are included in the article material, further inquiries can be directed to the corresponding author.

Funding

This study was supported by the National Natural Science Foundation of China (No. 81873762), the Hunan Provincial Natural Science Foundation of China (2022SK2032, 2022JJ40699), and the Science and Technology Planning Project of Changsha (No. kq2202407). The funders had no role in the design of the study and collection, analysis, decision to publish, interpretation of data or preparation of the manuscript.

Declaration of competing interest

The authors declare that they have no known competing financial interests or personal relationships that could have appeared to influence the work reported in this paper.

References

[1] Staudt Keli Jaqueline, Bruna Bernar Dias, Alves Izabel Almeida, et al., Modeling and simulation as a tool to assess voriconazole exposure in the central nervous system, Pharmaceutics 15 (7) (2023) 1781, https://doi.org/10.3390/pharmaceutics15071781.
[2] Laya Reddy, George R. Thompson, Koff Alan, et al., Entrapment syndrome in a kidney transplant recipient with cryptococcal meningitis, Pathogens 12 (5) (2023) 711, https://doi.org/10.3390/pathogens12050711.
[3] Lee Hiu Ham, Carmichael Dylan J, Rîbeiro Victoria, et al., Glucuronoxylomannan intranasal challenge prior to Cryptococcus neoformans pulmonary infection enhances cerebral cryptococcosis in rodents, PLoS Pathog. 19 (4) (2023) e1010941, https://doi.org/10.1371/journal.ppat.1010941.
[4] Thak Eun Jung, Son Ye Ji, Lee Dong-Jik, et al., OExtension of -linked mannosylation in the Golgi apparatus is critical for cell wall integrity signaling and interaction with host cells in cryptococcus neoformans pathogenesis, mBio 13 (6) (2022) e0211222, https://doi.org/10.1128/mbio.02112-22.
[5] J. Kim, K.T. Lee, J.S. Lee, J. Shin, B. Cui, K. Yang, et al., Fungal brain infection modelled in a human-neurovascular-unit-on-a-chip with a functional blood-brain barrier, Nat. Biomed. Eng. 5 (8) (2021) 830–846, https://doi.org/10.1038/s41551-021-00743-8.
[6] Y.H. Woo, L.R. Martinez, *Cryptococcus neoformans*-astrocyte interactions: effect on fungal blood brain barrier disruption, brain invasion, and meningitis progression, Crit. Rev. Microbiol. 47 (2) (2021) 206–223, https://doi.org/10.1080/1040841X.2020.1869178.
[7] J. Chen, X. Wang, J. Hu, J. Du, C. Dordoe, Q. Zhou, et al., FGF20 protected against BBB disruption after traumatic brain injury by upregulating junction protein expression and inhibiting the inflammatory response, Front. Pharmacol. 11 (2021) 590669, https://doi.org/10.3389/fphar.2020.590669 defined.
[8] C. Janke, M.M. Magiera, The tubulin code and its role in controlling microtubule properties and functions, Nat. Rev. Mol. Cell Biol. 21 (6) (2020) 307–326, https://doi.org/10.1038/s41580-020-0214-3.
[9] D. Khilazheva Elena, I. Mosiagina Angelina, A. Panina Yulia, et al., Impact of NLRP3 depletion on aging-related metaflammation, cognitive function, and social behavior in mice, Int. J. Mol. Sci. 24 (23) (2023) 16580, https://doi.org/10.3390/ijms242316580.

[10] Chengli Liu, Kun Yao, Tian Qi, et al., CXCR4-BTK axis mediate pyroptosis and lipid peroxidation in early brain injury after subarachnoid hemorrhage via NLRP3 inflammasome and NF-κB pathway, Redox Biol. 68 (undefined) (2023) 102960, https://doi.org/10.1016/j.redox.2023.102960.
[11] C. Qiao, Q. Zhang, Q. Jiang, T. Zhang, M. Chen, Y. Fan, et al., Inhibition of the hepatic Nlrp3 protects dopaminergic neurons via attenuating systemic inflammation in a MPTP/p mouse model of Parkinson's disease, J. Neuroinflammation 15 (1) (2018) 193, https://doi.org/10.1186/s12974-018-1236-z.
[12] L.G. Danielski, A.D. Giustina, S. Bonfante, M.P. de Souza Goldim, L. Joaquim, K.L. Metzker, et al., NLRP3 activation contributes to acute brain damage leading to memory impairment in sepsis-surviving rats, Mol. Neurobiol. 57 (12) (2020) 5247–5262, https://doi.org/10.1007/s12035-020-02089-9.
[13] Y. Huang, W. Xu, R. Zhou, NLRP3 inflammasome activation and cell death, Cell. Mol. Immunol. 18 (9) (2021) 2114–2127, https://doi.org/10.1038/s41423-021-00740-6.
[14] M. Ridge Karen, John E. Eriksson, Milos Pekny, et al., Roles of vimentin in health and disease, Genes Dev. 36 (7–8) (2022) 391–407, https://doi.org/10.1101/gad.349358.122.
[15] H. Zhu, Y. Cao, W. Su, S. Huang, W. Lu, Y. Zhou, et al., Enterovirus A71 VP1 variation A289T decreases the central nervous system infectivity via attenuation of interactions between VP1 and vimentin in vitro and in vivo, Viruses 11 (5) (2019) 467, https://doi.org/10.3390/v11050467.
[16] K. Ireton, R. Mortuza, G.C. Gyanwali, A. Gianfelice, M. Hussain, Role of internalin proteins in the pathogenesis of Listeria monocytogenes, Mol. Microbiol. 116 (6) (2021) 1407–1419, https://doi.org/10.1111/mmi.14836.
[17] W. Luo, J. Zhong, W. Zhao, J. Liu, R. Zhang, L. Peng, et al., Proteomic analysis of human brain microvascular endothelial cells reveals differential protein expression in response to enterovirus 71 infection, BioMed Res. Int. 2015 (defined) (2015) 864169, https://doi.org/10.1155/2015/864169.
[18] M. Masomian, S. Lalani, C.L. Poh, Molecular docking of SP40 peptide towards cellular receptors for enterovirus 71 (EV-A71), Molecules 26 (21) (2021) 6576, https://doi.org/10.3390/molecules26216576.
[19] Hao Pengfei, Qiaoqiao Qu, Zhaoxia Pang, et al., Interaction of species A rotavirus VP4 with the cellular proteins vimentin and actin related protein 2 discovered by a proximity interactome assay, J. Virol. 97 (12) (2023) e0137623, https://doi.org/10.1128/jvi.01376-23.
[20] G. dos Santos, M.R. Rogel, M.A. Baker, J.R. Troken, D. Urich, L. Morales-Nebreda, et al., Vimentin regulates activation of the NLRP3 inflammasome, Nat. Commun. 6 (2015) 6574, https://doi.org/10.1038/ncomms7574, defined).
[21] G.S. Sethi, S. Sharma, A.S. Naura, PARP inhibition by olaparib alleviates chronic asthma-associated remodeling features via modulating inflammasome signaling in mice, IUBMB Life 71 (7) (2019) 1003–1013, https://doi.org/10.1002/iub.2048.
[22] X. He, X. Shi, S. Puthiyakunnon, L. Zhang, Q. Zeng, Y. Li, et al., CD44-mediated monocyte transmigration across Cryptococcus neoformans-infected brain microvascular endothelial cells is enhanced by HIV-1 gp41-I90 ectodomain, J. Biomed. Sci. 23 (2016) 28, https://doi.org/10.1186/s12929-016-0247-2, defined.
[23] L.K. Zhang, J.W. Qiu, X.L. Liang, B.Y. Huang, Y. Li, L. Du, et al., Role of CD44 in monocyte transmigration across Cryptococcus neoformans-infected blood-brain barrier in vitro, Nan Fang Yi Ke Da Xue Xue Bao 35 (4) (2015) 468–473. Chinese. PMID: 25907927.
[24] J. Zhao, W. Weng, C. Chen, J. Zhang, The prevalence and mortality of cryptococcal meningitis in patients with autoimmune diseases: a systematic review and meta-analysis, Eur. J. Clin. Microbiol. Infect. Dis. 40 (12) (2021) 2515–2523, https://doi.org/10.1007/s10096-021-04293-4.
[25] Kim Jin, Lee Kyung-Tae, Lee Jong Seung, et al., Fungal brain infection modelled in a human-neurovascular-unit-on-a-chip with a functional blood-brain barrier, Nat. Biomed. Eng. 5 (8) (2021) 830–846, https://doi.org/10.1038/s41551-021-00743-8.
[26] O. Zaragoza, Basic principles of the virulence of *Cryptococcus*, Virulence 10 (1) (2019) 490–501, https://doi.org/10.1080/21505594.2019.1614383.
[27] F. Yang, Z. Wang, X. Wei, H. Han, X. Meng, Y. Zhang, et al., NLRP3 deficiency ameliorates neurovascular damage in experimental ischemic stroke, J. Cerebr. Blood Flow Metabol. 34 (4) (2014) 660–667, https://doi.org/10.1038/jcbfm.2013.242.
[28] D.Y. Fann, S.Y. Lee, S. Manzanero, S.C. Tang, M. Gelderblom, P. Chunduri, et al., Intravenous immunoglobulin suppresses NLRP1 and NLRP3 inflammasome-mediated neuronal death in ischemic stroke, Cell Death Dis. 4 (9) (2013) e790, https://doi.org/10.1038/cddis.2013.326.
[29] Z. Yang, L. Zhong, R. Xian, B. Yuan, MicroRNA-223 regulates inflammation and brain injury via feedback to NLRP3 inflammasome after intracerebral hemorrhage, Mol. Immunol. 65 (2) (2015) 267–276, https://doi.org/10.1016/j.molimm.2014.12.018.
[30] Y. Dong, C. Fan, W. Hu, S. Jiang, Z. Ma, X. Yan, et al., Melatonin attenuated early brain injury induced by subarachnoid hemorrhage via regulating NLRP3 inflammasome and apoptosis signaling, J. Pineal Res. 60 (3) (2016) 253–262, https://doi.org/10.1111/jpi.12300.
[31] S. Alfonso-Loeches, J. Ureña-Peralta, M.J. Morillo-Bargues, U. Gómez-Pinedo, C. Guerri, Ethanol-induced TLR4/NLRP3 neuroinflammatory response in microglial cells promotes leukocyte infiltration across the BBB, Neurochem. Res. 41 (1–2) (2016) 193–209, https://doi.org/10.1007/s11064-015-1760-5.
[32] O.V. Chernikov, J.S. Moon, A. Chen, K.F. Hua, Editorial: NLRP3 inflammasome: regulatory mechanisms, role in health and disease and therapeutic potential, Front. Immunol. 12 (2021) 765199, https://doi.org/10.3389/fimmu.2021.765199 defined.
[33] C. Wu, M. Yang, R. Liu, H. Hu, L. Ji, X. Zhang, et al., Nicotine reduces human brain microvascular endothelial cell response to *Escherichia coli* K1 infection by inhibiting autophagy, Front. Cell. Infect. Microbiol. 10 (2020) 484, https://doi.org/10.3389/fcimb.2020.00484, defined.
[34] Q.S. Wang, H.G. Ding, S.L. Chen, X.Q. Liu, Y.Y. Deng, W.Q. Jiang, et al., Hypertonic saline mediates the NLRP3/IL-1β signaling axis in microglia to alleviate ischemic blood-brain barrier permeability by downregulating astrocyte-derived VEGF in rats, CNS Neurosci. Ther. 26 (10) (2020) 1045–1057, https://doi.org/10.1111/cns.13427.
[35] H.S. Manzer, R.I. Villarreal, K.S. Doran, Targeting the BspC-vimentin interaction to develop anti-virulence therapies during Group B streptococcal meningitis, PLoS Pathog. 18 (3) (2022) e1010397, https://doi.org/10.1371/journal.ppat.1010397.
[36] C.B. Victorio, Y. Xu, Q. Ng, V.T. Chow, K.B. Chua, Phenotypic and genotypic characteristics of novel mouse cell line (NIH/3T3)-adapted human enterovirus 71 strains (EV71:TLLm and EV71:TLLmv), PLoS One 9 (3) (2014) e92719, https://doi.org/10.1371/journal.pone.0092719.
[37] U. Wilhelmsson, L. Li, M. Pekna, C.H. Berthold, S. Blom, C. Eliasson, et al., Absence of glial fibrillary acidic protein and vimentin prevents hypertrophy of astrocytic processes and improves post-traumatic regeneration, J. Neurosci. 24 (21) (2004) 5016–5021.
[38] T. Toyooka, H. Nawashiro, N. Shinomiya, K. Shima, Down-regulation of glial fibrillary acidic protein and vimentin by RNA interference improves acute urinary dysfunction associated with spinal cord injury in rats, J. Neurotrauma 28 (4) (2011) 607–618, https://doi.org/10.1089/neu.2010.1520.
[39] S.H. Huang, F. Chi, L. Peng, T. Bo, B. Zhang, L.Q. Liu, et al., Vimentin, a novel NF-κB regulator, is required for meningitic Escherichia coli K1-induced pathogen invasion and PMN transmigration across the blood-brain barrier, PLoS One 11 (9) (2016) e0162641, https://doi.org/10.1371/journal.pone.0162641.